Detection of Lead Diffusion in Geological Samples using Rutherford Backscattering Spectrometry

By

Andrew Martin McCalmont

****

Submitted in partial fulfillment

of the requirement for

Honors in the Department of Physics and Astronomy

UNION COLLEGE

June 2016

Table of Contents

ABSTRACT

McCALMONT, ANDREW Detection of Lead Diffusion in Geological Samples using Rutherford Backscattering Spectrometry (RBS)

ADVISOR: LaBRAKE, SCOTT

A Rutherford Backscattering (RBS) analysis experiment was performed on several pyrrhotite samples in order to understand their lead (Pb) diffusive properties and determine the diffusion coefficients for Pb into the sample. The pyrrhotite samples were prepared at Rensselaer Polytechnic Institute and were subsequently annealed for one to several days at temperatures on the order of 500–800℃. A 1.1–MV Pelletron Accelerator in the Union College Ion Beam Analysis Laboratory was used to produce beams of 3.3–MeV alpha particles. The beam of alpha particles collided with the samples and the backscattered alpha particles' energies were detected using a silicon surface barrier detector. The backscattered alpha particle energy spectra were then analyzed using SIMNRA to determine the diffusivity of Pb in the samples. The simulated layers of the sample (obtained using SIMNRA) were determined using the collected RBS spectra and known diffusion trends. Three RBS spectra on the Pb–pyrrhotite samples were collected, simulated and diffusion coefficients D= $3.4\text{x}10^{-22}$ m^2/s, $5.6\text{x}10^{-21}$ m^2/s, and $1.1\text{x}10^{-20}$ m^2/s were determined. The activation energy can be described by the relation: $D = 1.0 \exp(-56 \text{ kJ mol}^{-1} / RT)$. These diffusion coefficients and activation energy were found to be consistent with prior results [1].

1. Introduction

1.1 Motivation and Background

Chronological dating of geological specimens or geochronology is an important aspect of geophysics. One aspect of geochronological analysis that has been investigated increasingly as of late is elemental diffusion, which is the process by which dissolved molecules and atoms move from a region of higher concentration to a region of lower concentration. In geological samples this may involve atoms diffusing deeper into the specimen from the surface. The idea of diffusion was first described by Adolf Eugen Fick, who also theorized what are now known as Fick's laws, which describe how concentration, temperature, and pressure affect the diffusion process [2]. As the specimen ages over time certain atoms and molecules diffuse deeper into the specimen, thus we can determine the approximate age of the specimen by measuring the concentrations those elements at various depths in the specimen. However as radiogenic lead is produced, it can diffuse away at high temperatures. Understanding the diffusion behavior allows us to determine the closure temperature, the temperature at which all the radiogenic lead stays in the sample. In our case, we examined how lead diffuses into FeS or pyrrhotite. However, in order to correctly determine the age of a geological sample, the diffusivity of a sample must be understood, namely a diffusion coefficient, which is a measure of how well other minerals can diffuse into the sample. The diffusivity of a system changes based upon the temperature and pressure it has been subjected to. This relationship is described the Arrhenius equation, first proposed by Svante Arrhenius [3].

One of the ways that the diffusion coefficients have been measured in prior research by H. Watson, E.B. Watson, and D.J. Cherniak at the Rensselaer Polytechnic Institute (RPI) has been through Rutherford backscattering spectrometry (RBS). By analyzing the resulting RBS

spectrum from an experimental sample, the diffusion properties of the given samples can be determined [4]. In this research we are mostly concerned with the diffusion coefficient of the lead in the sample in a method analogous to what Cherniak was able to measure in naturally occurring minerals such as: pyrrhotite, apatite, titanite, rutile, and zircon [4].

1.2 Rutherford Backscattering

Previous research in the Union College Ion Beam Analysis Laboratory has focused on proton-induced x-ray emission (PIXE) analysis of environmental samples. PIXE spectroscopy has poorer mass resolution for heavy elements, like lead. In this project it is more advantageous to use the ion beam analysis technique called Rutherford backscattering spectroscopy (RBS). RBS is ideal because it provides information about the concentration of trace elements that are heavier than the major components of a given sample. With RBS, high energy ions, such as alpha particles, bombard the sample [5]. A small number of the induced ions collide with the nuclei on the surface of the sample. These ions do not directly touch the nuclei, but rather interact via Coulombic forces, and can be modeled as elastic collisions in classical mechanics, as illustrated in Figure 1:

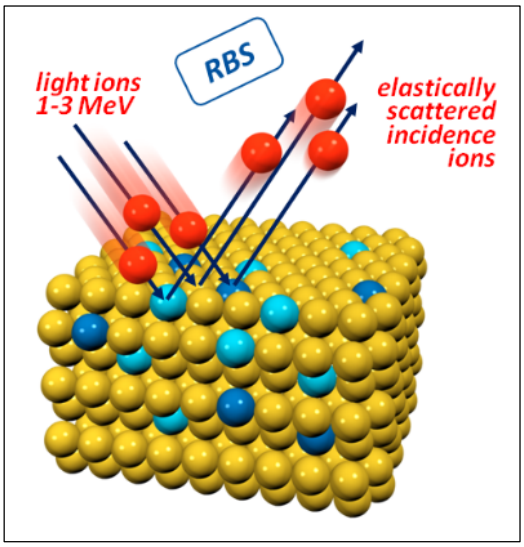

Figure 1: Cartoon image showing the elastic collision that occurs during Rutherford backscattering [6].

The majority of the incident ions end up imbedded in the specimen, however some ions do manage to scatter out of the sample almost nearly opposite to the direction of the incident ions. Since the energy of the projected ions dissipates the deeper the ions penetrate into the material, because of collisions with electrons and nuclei, the backscattered ions have less energy than the incident ions. The backscattered ions then bombard the detector which can distinguish ions of different energy amounts, for the given angle. The detector is connected to a computer, which counts the ions, binned by energy levels [5]. The resulting histogram of the number of alpha particles versus their energies is used in the analysis to determine the diffusion coefficients.

2. Procedure

2.1 Collection and Preparation of Samples

The samples in this project were pyrrhotite (FeS), which is similar to pyrite (FeS_2) in its chemical composition. The FeS came from the Bluebell mine in Canada. Watson prepared the samples by mixing FeS and PbS powders and pre-reacting them at temperatures in silica capsules at 500℃ for 24 hours. After they were pre-reacted, the samples were polished using 0.3-μm alumina powder and colloidal silica, resulting in polished flat surfaces that are ideal for RBS analysis. Next, the samples were cleaned using acetone. Then the samples were annealed in 1-atm furnaces in temperatures on the order of 500℃ to 850℃ for one to several days. The samples were then placed in the beamline of a 1.1–MV particle accelerator where they were bombarded by a beam of 3.3–MeV alpha particles.

2.2 Particle Accelerator

The particle accelerator used in this project was a National Electrostatics Corporation 1.1-MV tandem electrostatic particle accelerator. In this project we configured the accelerator to use alpha particles. Under this configuration a 100-MHz radio-frequency signal is applied to a quartz bottle of helium gas, creating a positive-ion plasma, since the electrons are stripped from the helium in the process [7]. The helium nuclei are accelerated out of the quartz bottle by a potential difference of 3.8 kV. After this initial acceleration, the helium nuclei pass though a low-density Rb vapor, where through charge exchange collision, they gain three electrons. This results in an He^- ion[7]. The ions then drift toward the accelerator tank seen in Figure 2.

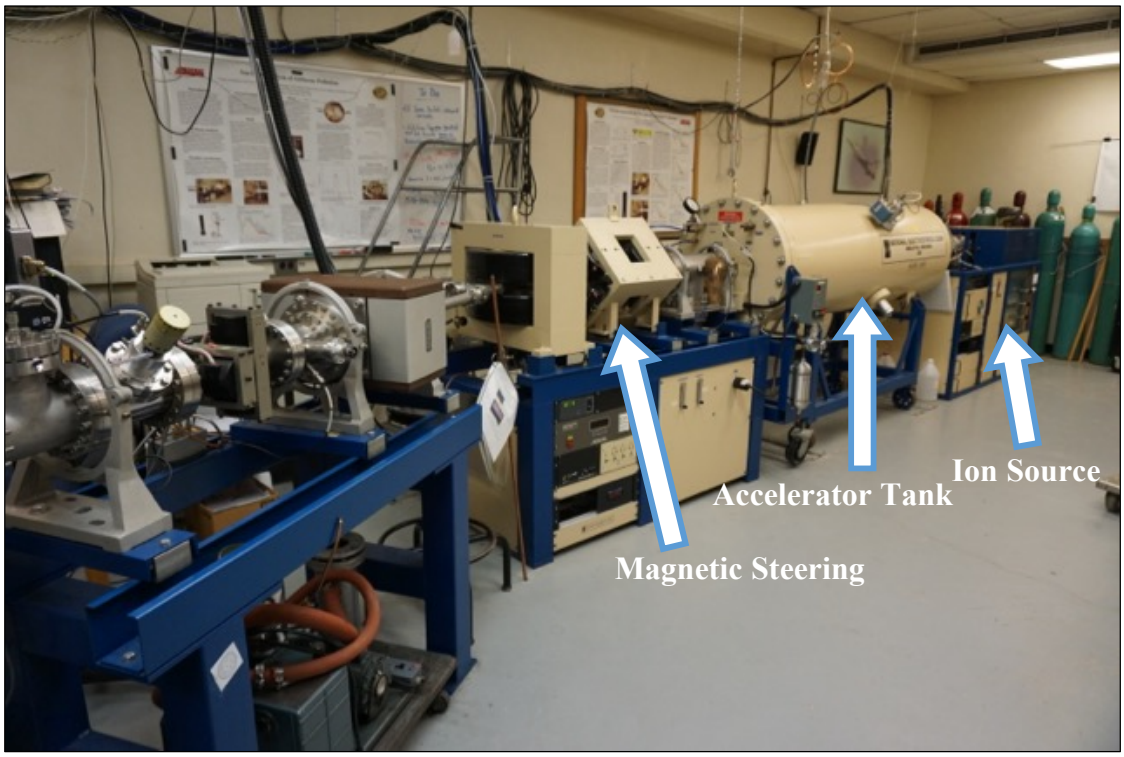

Figure 2: Photograph of the Union College 1.1-MV Pelletron accelerator. Particles originate in the ion source, are accelerated in tandem in the tank, and then are magnetically steered before heading to the scattering chamber shown in Figure 3.

The accelerator tank consists of three parts. From right to left in Figure 2, they are the low energy column, the terminal, and the high energy column. The first half or low-energy end of the accelerator has a potential difference of 1.1 MV with respect to the rightmost end of the tank and the terminal in the center of the tank, and 1.1 MeV of work is done on the alpha particles. When the alpha particles pass through the terminal they are stripped of their electrons by nitrogen gas and are accelerated away from the terminal. In the second half of the accelerator, the He^{2+} are accelerated via another potential difference of 1.1 MV and 2.2 MeV of work is performed on the alpha particles, resulting in a total of 3.3072 MeV (including the source) of

work done on the alpha particles. From the work done on the alpha particles we can determine the speed of their using the following equation:

$$W_{total} = KE_f - KE_i = 3.3072\ MeV = (\gamma - 1)m_\alpha c^2 \quad (1)$$

Solving this equation for γ and get 1.00089 and from the definition of γ we can solve for the speed of the alpha particle, 1.263×10^7 m/s. Since this speed is below the relativistic limit we do not have to worry about relativistic effects in our analysis.

In addition to the alpha particles, other charged objects (such as N, O, or Rb) get accelerated. To filter out the alpha particles from the charged particles, we magnetically steer the beam using a magnetic field. We pick a magnetic field to filter out the 3.3–MeV alpha particles and the other charges do not make the bend. After the particles are steered they reach the scattering chamber, where they collide with the sample and some alpha particles scatter in their incident direction. The end of the accelerator and the scattering chamber can be seen in Figure 3:

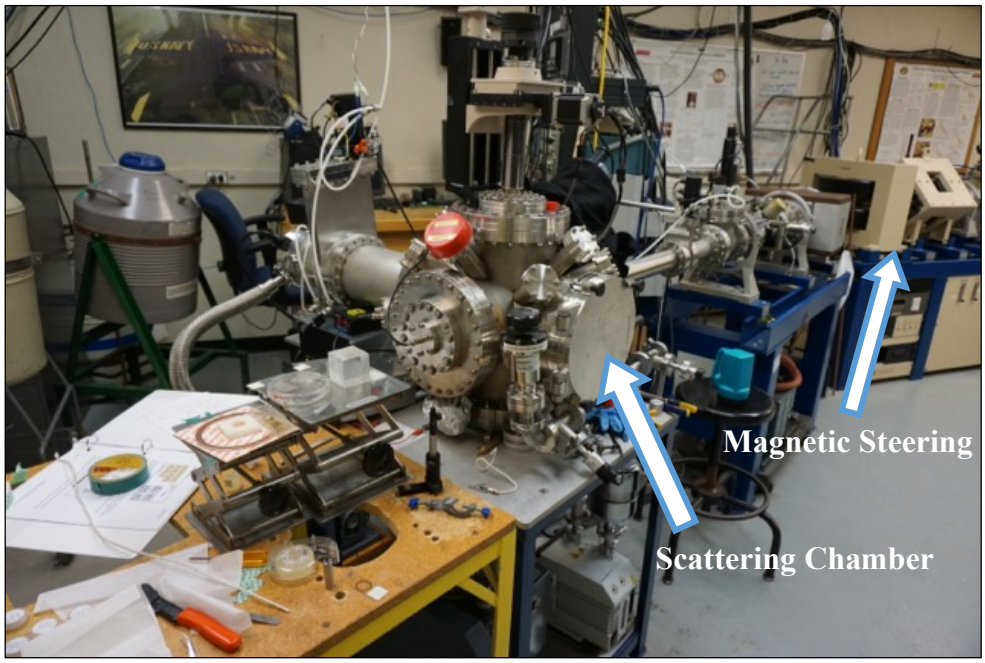

Figure 3: Image of the tail end of the accelerator. In this view, the scattering chamber can be seen.

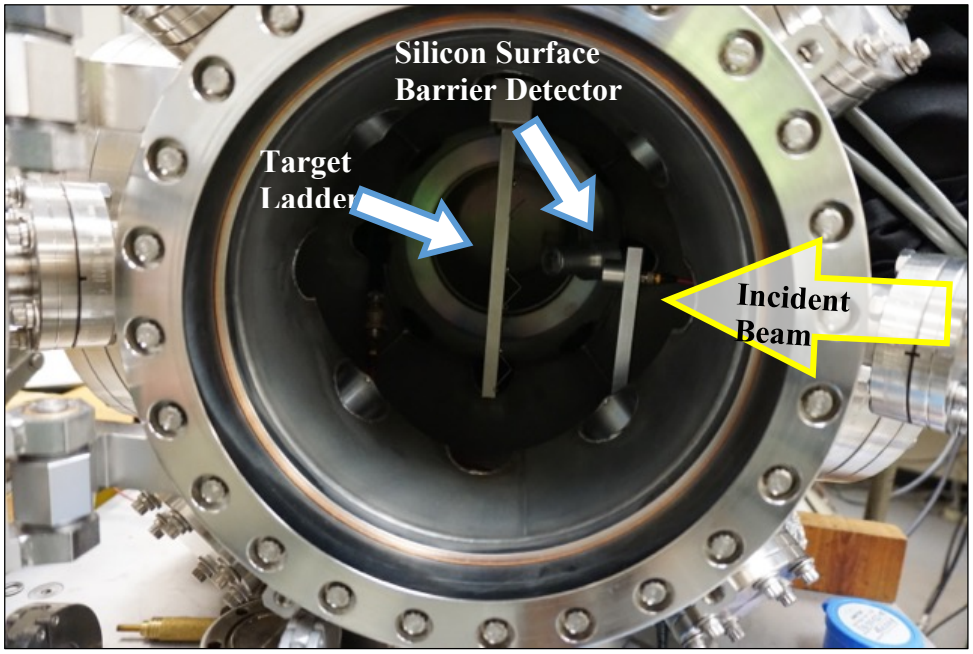

Figure 4: Image showing the accelerator scattering chamber, where the incident beam collides with the target.

The backscattered particles are detected by a silicon surface barrier detector shown in Figure 4, and thus the energies of the backscattered alpha particles and numbers of alpha particles are recorded. The scattering angle, the angle between the beamline and the detector in this setup was 160°. From the distribution of detected alpha particles, we can generate an RBS spectrum.

2.3 Data Analysis

The detectors were first calibrated using Au foil samples. Data on the number of alpha particles versus their channel number was collected using a software package called Maestro. Detector counts were collected by channel numbers, which correspond to different backscattered alpha particle energy levels using the calibration. By indicating the Au RBS spectra peaks in

Maestro, the energies of the scattered alpha particles could be matched to their respective channel numbers. Equation 2 shows the calibration used to covert the channel number to energy (in keV):

$$Energy = 5.914 \times (channel\ number) + 134.7. \quad (2)$$

Next, the pyrrhotite samples were placed in the scattering chamber and the RBS process was performed to obtain spectra. The resulting spectra data were imported into a software package called SIMNRA, which can simulate RBS spectra [8]. In SIMNRA, the sample is represented by the target configuration. A target can and will usually have many layers. The end user must specify the elemental composition each layer, in order for SIMNRA to correctly simulate an RBS spectrum [8]. In pure FeS, each target layer has a Fe and S fractional concentration of 0.5 and 0.5 respectively, where the total concentration must sum to 1 in a layer. Since the Pb substitutes for Fe in the crystal structure of FeS, the Pb concentrations in each layer were made to complement the fractional concentration of Fe, and thus together add up to a total fractional concentration of 0.5. The S in each layer remained at a fixed fractional concentration of 0.5, because in theory it is not effected by the diffusion of Pb into the sample. Additionally, the user must specify the experimental parameters, where the user must enter the energy profile of the ion beam, the angle of between the beam and the detector, and energy calibrations. There is some degree of subjectivity with getting SIMNRA to correctly generate an RBS spectra. SIMNRA quantifies layer thicknesses by an areal density in atoms/cm^2, which we converted to a thicknesses by Equation 3:

$$\Delta x = \frac{\rho_A}{\rho} \frac{M}{N_A} \quad (3)$$

where Δx is the layer thickness, ρ_A is the areal density of the layer in g/cm^2, ρ is the density of the sample in g/cm^3, M is the molar mass of the sample, and N_A is Avagdro's number. We found

it particularly useful to predict the correct layer concentrations of Pb by using the trend predicted by the diffusion equation:

$$C(x,t) = C_0\left[1 - \text{erf}\left(\frac{x}{\sqrt{4\,D\,t}}\right)\right] \quad (4)$$

where $C(x,t)$ is the fractional concentration of Pb in the layer, C_0 is the fractional concentration of Pb in the surface layer, x is the layer depth in the FeS sample, D is the diffusion coefficient, and t is the annealing time of the sample. We began by estimating a D and C_0, based on prior research with similar systems, in order to estimate the correct trend for the target layer concentrations and see how the SIMNRA fit compared to the experimental Pb profile. It was useful to guess a diffusion coefficient to control the width of the Pb profile fit and a C_0 value to control its height. After numerous iterations of using D and C_0, and once the SIMNRA fit closely matched the experimental Pb profile, we recorded the diffusion coefficient used to generate the fit. While this method initially sounds circular, diffusion coefficients were determined independently from known diffusion coefficients. Equation 4 was only used at this point to approximate the elemental concentration of target layers with the correct diffusion trend, and the initial D and C_0 were used to get an approximate fit, which we later refined for our data by varying these coefficients. We know from prior research that diffusion coefficients for Pb samples of this nature should be around magnitudes of 10^{-17} to 10^{-22} m^2/s [1].

Once the RBS data is correctly fit, we recorded the the lead concentrations for each layer. We recorded the concentrations of lead as a function of distance and input created a regression equation from this data. By linearizing the data with the inverse error function, since the data fit an error function trend, we were able to determine the line of best fit and thus determine the diffusion coefficient for the samples. It is also important to note that diffusion coefficients

measurements for this nature of research can easily be off by a factor of 3 from other measurements of the same sample and still be considered reasonable [1].

Lastly, the activation energy is what relates annealing temperature to a diffusion coefficient by way of the Arrhenius equation, shown in Equation 5. Annealing temperature determines the diffusivity of Pb into the sample:

$$D = D_0 \, e^{\frac{-E}{RT}} \tag{5}$$

where D is the diffusion coefficient, D_0 is the initial diffusion coefficient, E is the activation energy and T is the absolute temperature in Kelvin, and R is the gas constant [2]. The Arrhenius equation, Equation 5, was linearized, hence plotting the natural log of each sample's respective diffusion coefficient against the inverse of the annealing temperature of each sample, which is called an Arrhenius plot [9]. The activation energy was determined from the line of best fit from the Arrhenius plot.

3. Results and Analysis

3.1 Union Data

Using the apparatus described in the procedure section 2.2, I obtained multiple RBS spectra for the first pyrrhotite sample, PbPh5, as illustrated in Figure 5, where the energy axis is determined from Equation 2:

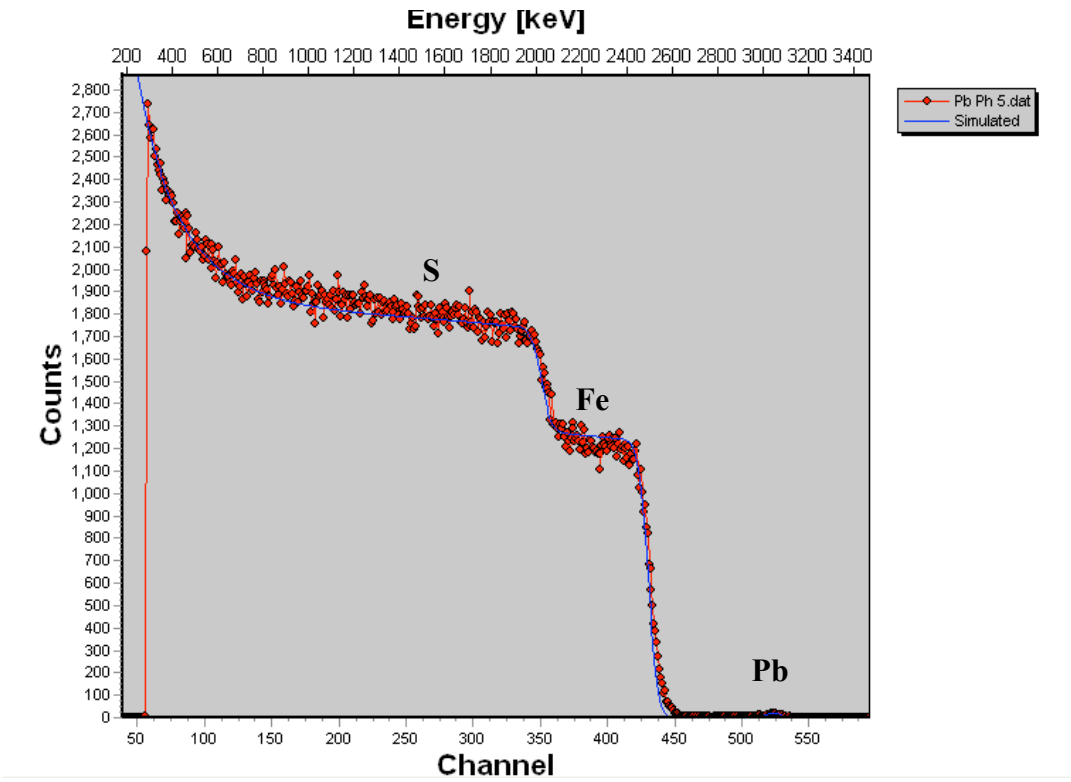

Figure 5: RBS spectrum representing pyrrhotite sample PbPh5. The backscattered alpha particle counts are plotted against the channel numbers, which correspond to alpha particle energy levels. The red points and line represent experimental data and the blue line represents the fit in SIMNRA.

The first plateau on the left in Figure 5 represents the S in the sample and the lower plateau on the right represents the heavier Fe. Heaver elements appear as peaks rather than plateaus, and it is for this reason that RBS is best used for heavy element analysis. The Pb in this view, around

channel 525, is barely visible, due to its low concentration, and can be seen better in the view in Figure 6:

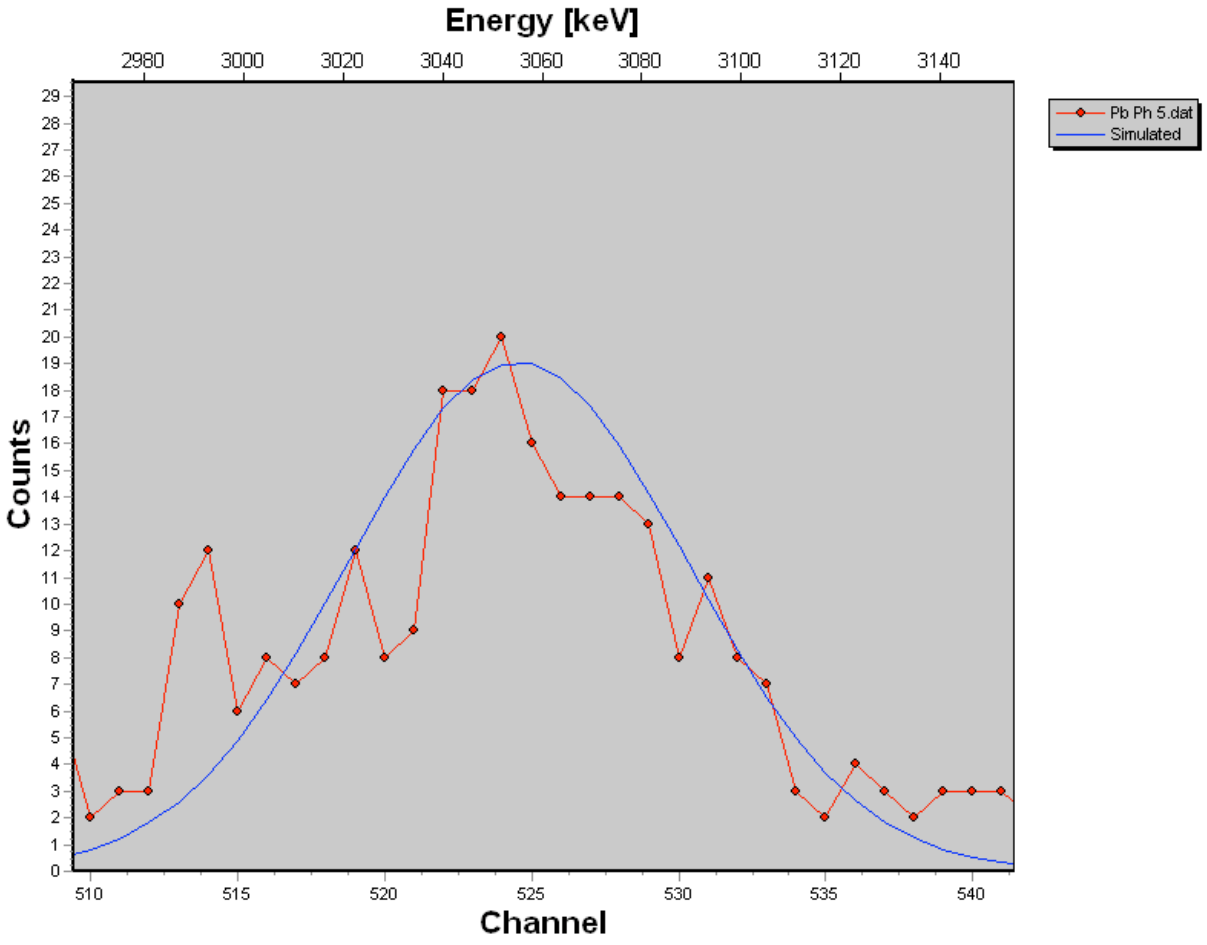

Figure 6: RBS Spectrum representing the first pyrrhotite sample, PbPh5, expanded in to show the profile of the Pb peak. The red points represent experimental data, and the blue curve is the SIMNRA fit.

In Figure 6, the expanded spectrum around channels 500 – 550 highlights the limited resolution of the obtained spectrum. We ran the accelerator for approximately 1.5 hours, which potentially limited the number of counts we saw in the Pb profile. Ideally, there should be more particle counts in the Pb peak in order to produce a more distinguishable Pb profile. Table 1

shows the Pb layer thicknesses, used in SIMNRA to generate the profile seen in Figure 5, and thus directly correspond to the distribution of alpha particle counts in the Pb profile:

Layer	Areal Density (10^{15} atoms/cm^2)	Concentration (fraction)
1	10	0.012500
2	10	0.011500
3	10	0.009500
4	10	0.008000
5	10	0.006500
6	10	0.005000
7	10	0.004000
8	60	0.000650
9	70	0.000040
10	80	0.000001

Table 1: The areal densities, which are used to determine layer depth, and the concentrations of Pb in each simulated layer of the pyrrhotite. These values were used in SIMNRA to generate a simulated spectrum.

Using Equation 3, the densities were converted into depths, which are then used in Figure 7, the depth profile of this pyrrhotite sample, which tells how the Pb concentration decreases as we proceed deeper into the sample:

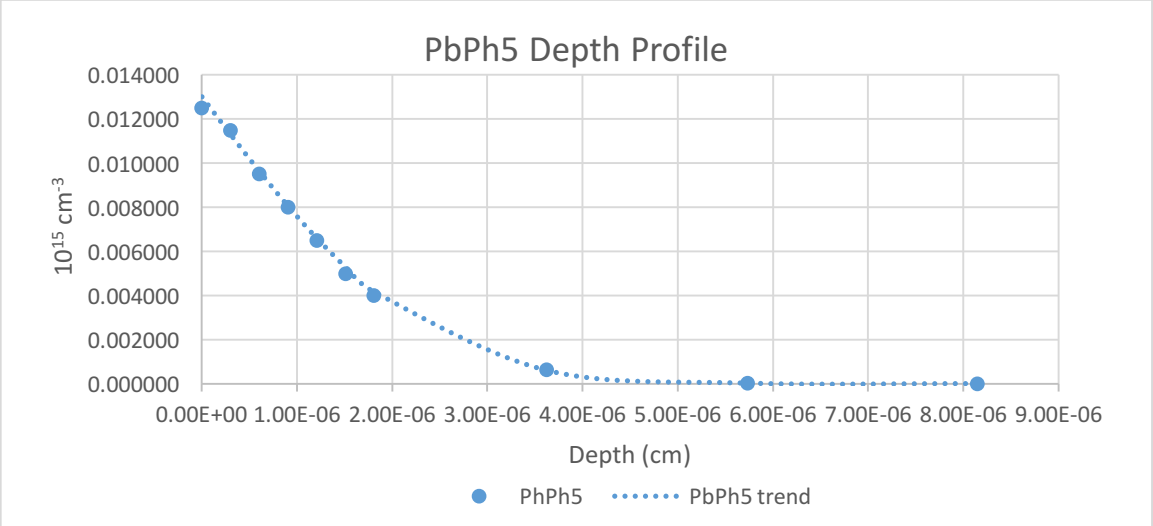

Figure 7: Depth profile of the pyrrhotite sample PhPb5, where depth is plotted against the Pb concentration for each layer of the pyrrhotite. The hashed line represents the error function trend predicted by the experimental value of *D*.

As per Equation 6, we can linearize the data by plotting $\text{erf}^{-1}\left[\frac{C_0-C}{C_0}\right]$ against the layer depth in Excel, as illustrated in Figure 8:

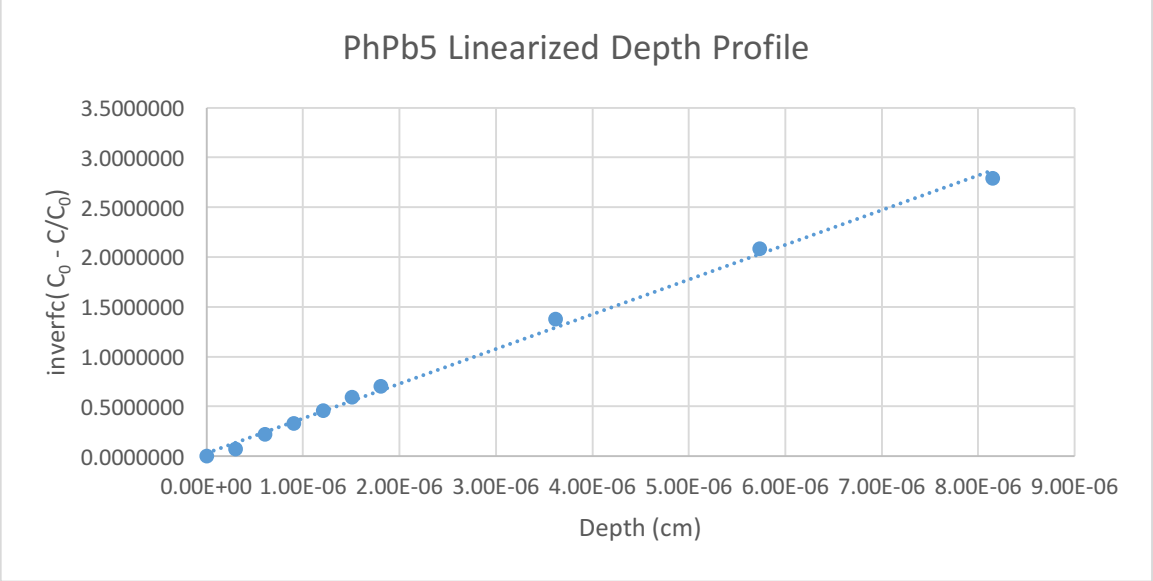

Figure 8: Depth is plotted against the inverse error function of the concentration to yield the linearized depth profile of the PbPh5, which can be used to determine D, the diffusion coefficient.

We know from Equation 4 that the slope of the linearized function represents $\frac{1}{\sqrt{4\,D\,t}}$, thus if know the annealing time we can solve for the diffusion coefficient. We know that the PbPh5 sample was annealed for 612,600 seconds (7.2 days) at a temperature of 557°C, thus we determined the diffusion coefficient of PbPh5 to be 3.4×10^{-22} m^2/s, which is 24% greater than the diffusion coefficient determined by H. Watson, 2.7×10^{-22} m^2/s.

A week later we performed a run with the same PbPh5 to see if we could detect a clearer RBS spectrum. The second run of the PbPh5 sample did not yield a discernable Pb profile, because there were not sufficient alpha particle counts in the Pb region of the RBS spectrum. We also attempted to acquire an RBS spectrum for another pyrrhotite sample, PhPb7, which was annealed for 22 hours at 702°C. The RBS spectrum expanded to show only the Pb profile for PhPb7 is illustrated in the following figure:

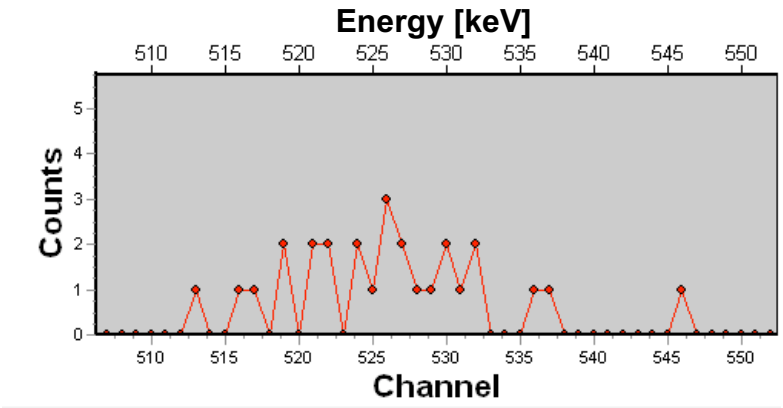

Figure 9: RBS Spectrum representing the second pyrrhotite sample, PbPh7, expanded in to show the profile of the Pb peak.

The profile for PbPh7 in Figure 9 has even more limited resolution than the PhPb5 sample, and thus I was unable to perform a fit spectrum with this sample of PbPh7.

3.2 Rensselaer Data

In coordination with H. Watson, we acquired RBS spectra from two samples samples, PbPh7 and PbPh8, again prepared at the Rensselaer Polytechnic Institute, but analyzed instead at the University at Albany. I used these RBS spectra to initially test out my process for profile fitting in SIMNRA and determining the diffusion coefficients. In the following figure we can see the Pb profile for the PbPh7 sample:

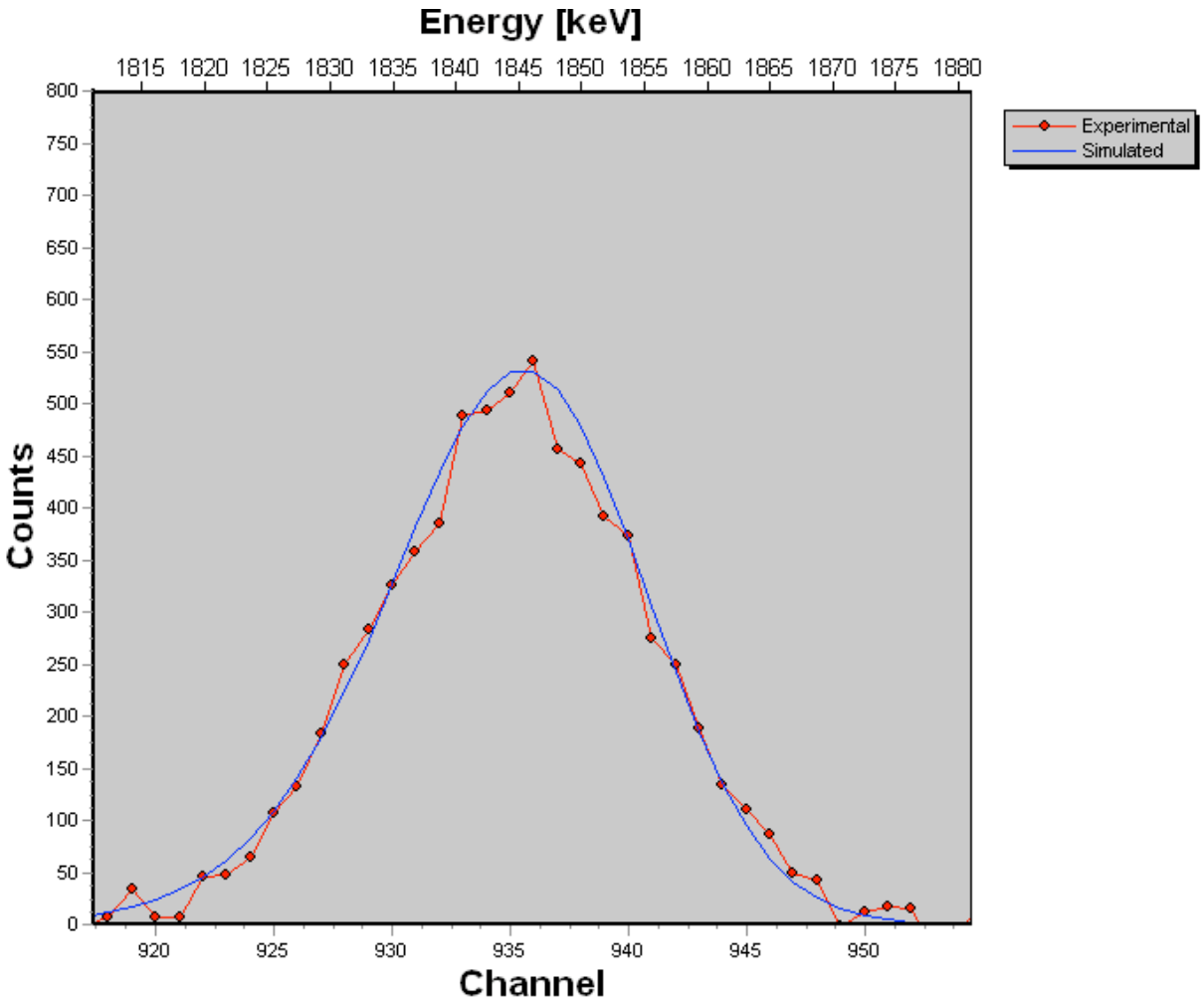

Figure 10: The RBS spectra for the PbPh7 sample expanded to show the profile for Pb. The blue line represents the simulated profile in SIMNRA.

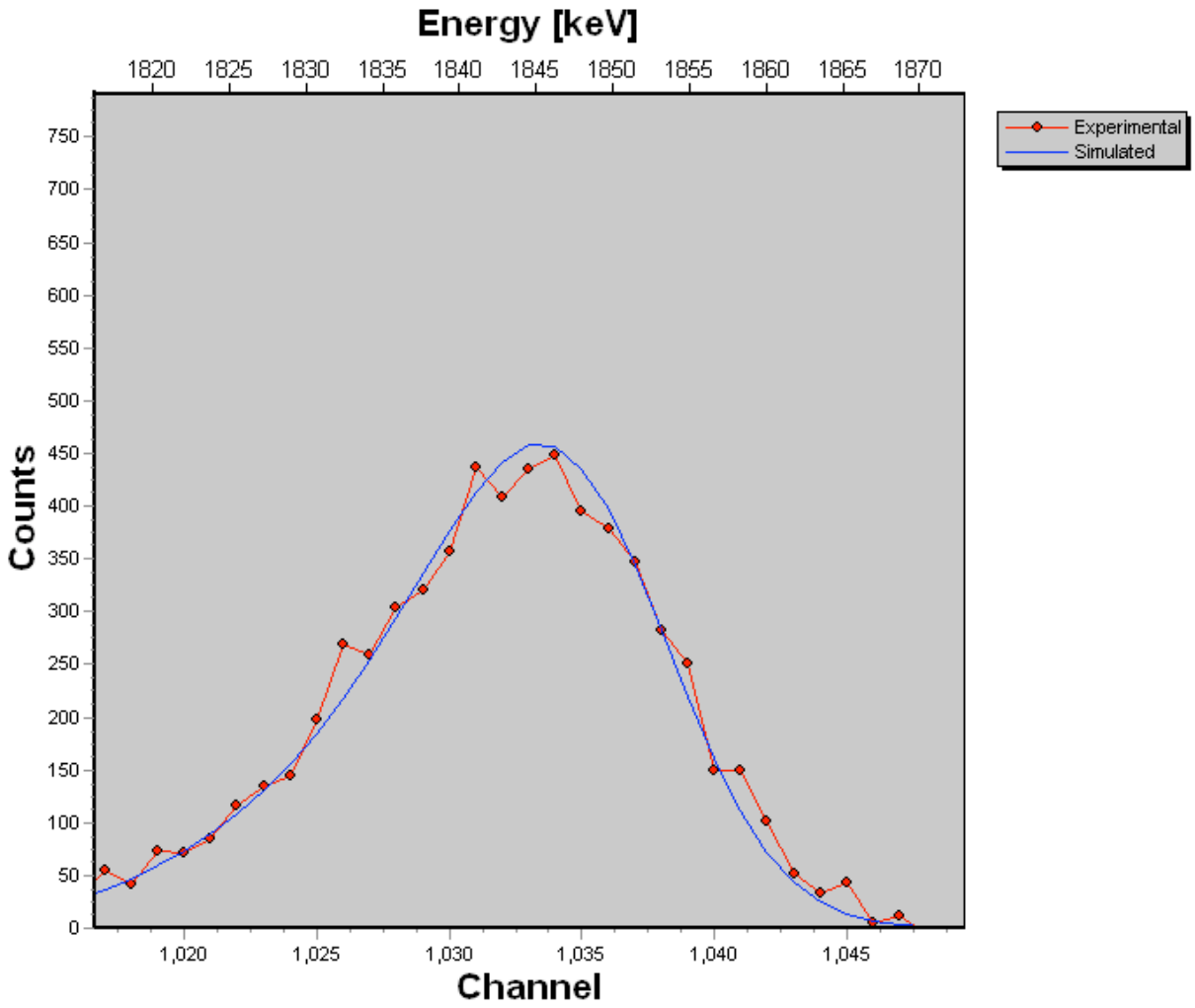

Figure 11: The RBS spectra for the PbPh8 sample expanded to show the profile for Pb. The blue line represents the simulated profile in SIMNRA.

The spectra in Figures 10 and 11 highlight that the RPI team was able to detect Pb profiles with significantly higher resolution than we were able to, perhaps due to longer run times or better beam alignment. The RPI team bombarded these samples for approximately 1 to 2 hours with 2–MeV alpha particles, and the scattering angle was 169.87°. These samples were fit using the target layer concentrations in Table 2:

Sample	PhPb7		PhPb8	
Layer	Areal Density (10^{15} atoms/cm^2)	Concentration (fraction)	Areal Density (10^{15} atoms/cm^2)	Concentration (fraction)
1	10	0.003600	10	0.002600
2	10	0.003200	10	0.002500
3	10	0.003000	10	0.002300
4	10	0.002700	10	0.002100
5	10	0.002400	10	0.002000
6	10	0.002100	10	0.001900
7	10	0.001900	10	0.001800
8	60	0.000800	60	0.001050
9	70	0.000200	70	0.000450
10	80	0.000020	80	0.000150

Table 2: The areal densities and the concentrations of Pb in each simulated layer of the pyrrhotite samples PhPb7 and PhPb8.

The densities and concentrations of the layers of the Pb in the FeS were again used in SIMNRA to generate the spectra seen in Figures 11 and 12. Figures 12 and 13 illustrate the depth profile for the PbPh7 sample:

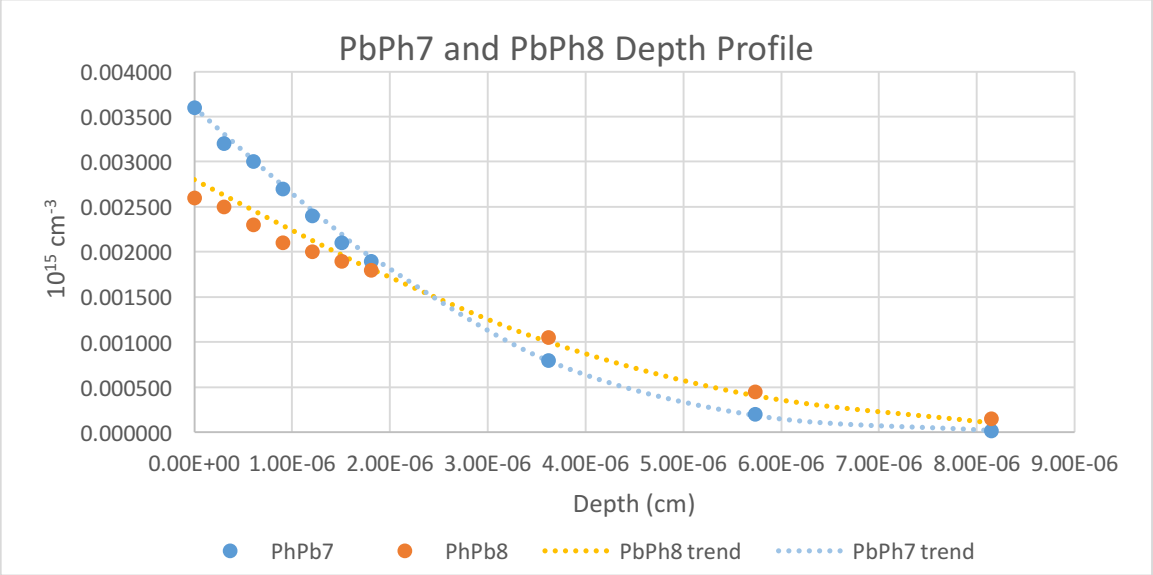

Figure 12: Depth profile of the pyrrhotite samples PbPh7 and PbPh8, where depth is plotted against the Pb concentration for each pyrrhotite layer. The trend lines show where the Pb concentrations should fall according to the experiential diffusion coefficient.

Again, I linearized the depth profile to acquire the diffusion coefficient, as illustrated in the following figure:

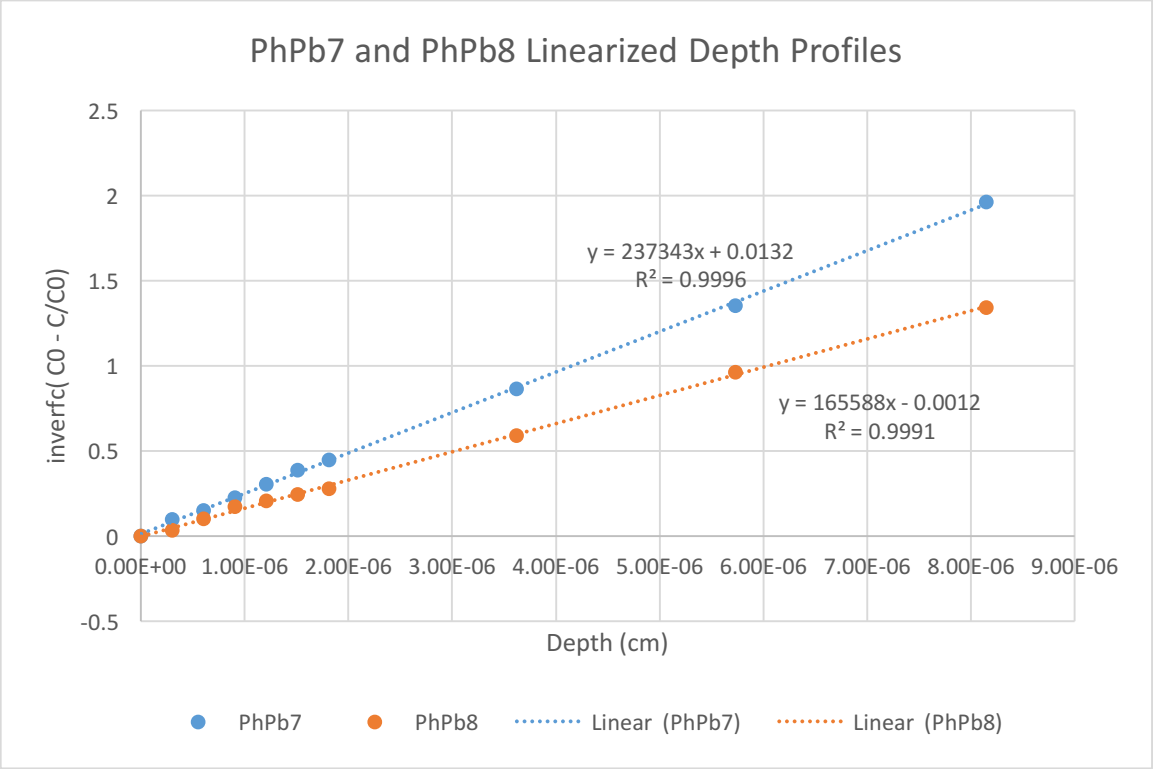

Figure 13: Depth is plotted against the inverse error function of the concentration, which can be used to determine D, the diffusion coefficient of the two samples.

We know that PhPb7 was annealed for 79200 seconds, and by using the previously described methods, we determined the diffusion coefficient of PhPb7 to be 5.6×10^{-21} m^2/s. This value is 143% greater than the one determined by Watson, 2.3×10^{-21} m^2/s. The PhPb8 sample was annealed for 86400 seconds, and we determined that its diffusion coefficient was 1.1×10^{-20} m^2/s. This is 340% greater than Watson's value of 2.5×10^{-21} m^2/s. Again, as I mentioned before, results that differ by a factor of 2 or 3 are considered reasonable for the nature of this research, since the magnitudes of the diffusion coefficients are what ultimately have the greatest effect in the determination of the activation energy.

3.3 Activation Energy

After the diffusion coefficients are determined, we can determine the activation energy of Pb by creating an Arrhenius plot, which plots the natural log of the respective sample's diffusion coefficient against the inverse of annealing temperature, as illustrated in Figure 14:

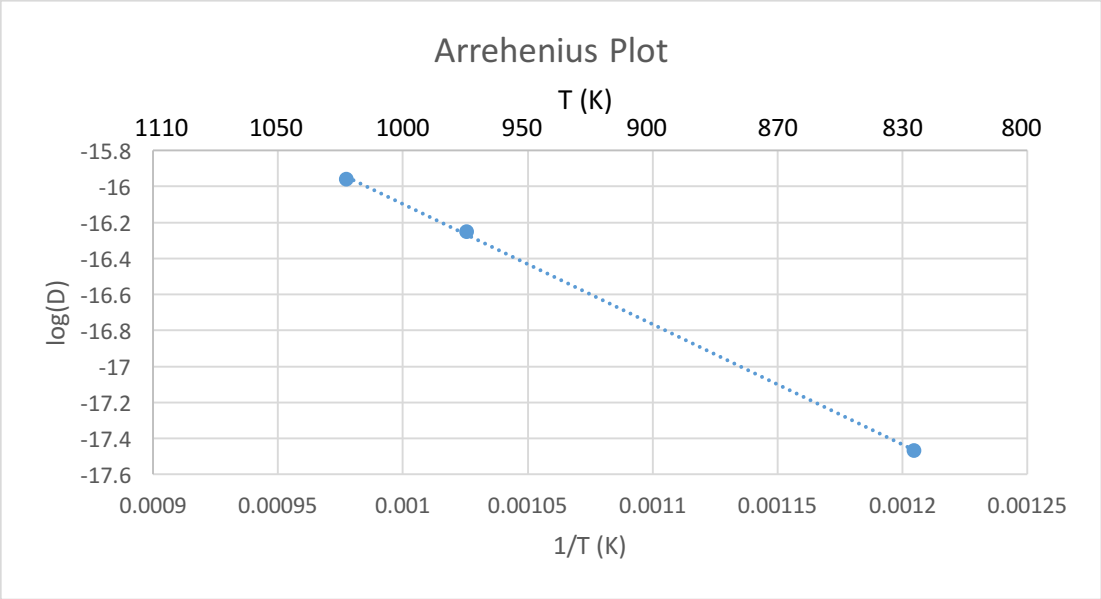

Figure 14: The Arrhenius plot for the three pyrrhotite samples. The regression equation slope can be used to derive the activation energy of the Pb in the FeS compound.

Figure 14 also shows that the diffusion coefficients strongly agree with the trend predicted by the linearized Arrhenius equation:

$$\text{Log}\, D = \text{Log} D_0 - \left(\frac{E}{R}\frac{1}{T}\right). \tag{8}$$

where, again, D is the diffusion coefficient, D_0 is the initial diffusion coefficient, E is the activation energy and T is the absolute temperature (usually in Kelvin). By determining the slope of the line of best fit in the Arrhenius plot in Figure 14, and then solving for E in Equation 8, we determined the activation energy of Pb in the pyrrhotite system to be 56 kJ/mol, which is 31% less than Watson's value of 81 kJ/mol. The activation energy can be described by the relation: $D = 1.0 \exp(-56 \text{ kJ mol}^{-1} / RT)$.

4. Conclusion

Our primary goal for this project was to determine the diffusion coefficient of the Pb in the FeS system and also implement the diffusion analysis methods at the Union College Ion-Beam Analysis Lab that were used in prior research by H. Watson and D.J. Cherniak. We determined the diffusion coefficients of the PbPh5, PbPh7, and PbPh8 samples from RPI to be 3.4×10^{-22} m^2/s, 5.6×10^{-21} m^2/s, and 1.1×10^{-20} m^2/s respectively. These values were all within agreement with the values determined by D.J. Cherniak and H. Watson. We also determined that the activation energy of Pb in the Pb–FeS system was 56 kJ/mol, which is 31% less than the RBI value. The activation energy can be described by the relation: $D = 1.0 \exp(-56 \text{ kJ mol}^{-1} / RT)$.

With the accelerator in working order, in future research, we will perform more runs on multiple samples. Performing longer runs and using samples with higher concentrations of Pb might also increase the size and quality of the resultant profiles. It would be wise to devise a more quantitative way to measure the accuracy of spectra fits. The current fit process in SIMNRA has a certain degree of subjectivity, since was possible to generate fits using layer concentrations that did not match the trends of the diffusion equation, Equation 6.

Thus despite problems arising from the detector resolution, we were able to acquire a Pb profile in a pyrrhotite spectrum. Our values for PhPh5 differed from the RPI values by 24%, thus we were able to analyze this spectrum with modest results. Additionally, we were able to analyze the respective RBS spectra for PbPh7 and PbPh8 with reasonable accuracy. We have also determined how to incorporate SIMNRA into our RBS analysis. More importantly, we have finalized the details of how to analyze the diffusivity of geological samples in further research at Union College.

5. References

[1] D.J. Cherniak. *Lead diffusion in titanite and preliminary results on the effects of radiation damage on Pb transport*. Chemical Geology Vol. 110., pp. 177–194. 1993.

[2] Zoltán Erdélyi. *Diffusion on the nanoscale: Volume diffusion*. http://web.unideb.hu/zerdelyi/diffusion-on-the-nanoscale/.

[3] Jim Clark. *Rate Constants and the Arrhenius Equation*. http://www.chemguide.co.uk/physical/basicrates/arrhenius.html. Oct 2013.

[4] E. Bruce Watson. *Diffusion Studies in Minerals*. SUNY Albany. http://www.albany.edu/ionbeamlab/research/programs/IBL_diffusion.shtml

[5] Evans Analytical Group. *RBS Theory*. http://www.eag.com/mc/rbs-theory.html

[6] Diagram modified from: https://www.hzdr.de/db/Cms?pOid=29856&pNid=3537

[7] National Electrostatic Corporation. http://www.pelletron.com/tutor.htm

[8] Matej Mayer. *SIMNRA User's Guide*. Max-Planck-Institut für Plasmaphysik. http://home.rzg.mpg.de/~mam/Manual.pdf. 2011.

[9] *Activation Energy*. Florida State University. http://www.chem.fsu.edu/chemlab/chm1046course/activation.html